A comparison of small signal modulation parameter extraction techniques for vertical-cavity, surface-emitting lasers

Christopher J. O'Brien, Marian M. Majewski, and Aleksandar D. Rakic

Abstract— **The small signal modulation characteristics of a vertical-cavity, surface-emitting laser (VCSEL) are determined using three different measurements: relative intensity noise, frequency response, and high resolution optical spectra. The resonant and damping frequencies were measured, and related rate equation parameters were extracted; excellent agreement was found both between experiment and theory, and amongst the different measurement techniques. The results and procedures are compared, and the findings are presented below.**

I. Introduction

Vertical-Cavity, Surface-Emitting Lasers (VCSELs) have grown greatly in popularity and capability. Unlike conventional edge-emitting devices, VCSELs are designed with a very short resonant cavity, which suppourts a single longitudinal mode; light is emitted perpendicularly to the plane of crystal growth, allowing the construction of two-dimensional transmitter arrays for high bandwidth-density applications. VCSELs have low threshold currents, high efficiencies, and can be tested on the wafer - minimising manufacturing costs.

VCSELs are heavily employed in high-bandwidth communications applications, and are particularly attractive candidates for use in optical interconnects. The maximum rate of direct modulation is limited by the interplay between photons and electrons, and can be described by the rate equations, which are characterised by a second order frequency response [1], [2]:

$$\frac{P(f)}{P_0} = \frac{f_r^2}{f_r^2 - f^2 + j\Gamma_d \frac{f}{2\pi}} \qquad (1)$$

$$\Gamma_d = \frac{1}{2\tau_n} + Kf_r^2 \qquad (2)$$

$$K = 2\pi^2(\tau_p + \tau_c) \qquad (3)$$

$$f_r = D\sqrt{P} \qquad (4)$$

where, τ_p is the photon lifetime, τ_n is the carrier lifetime, τ_c is a lumped rate equation parameter, P is the optical power, f_r is the resonant frequency, and Γ_d is the damping frequency. These relationships indicate that a laser's high frequency response improves at high drive currents, and that the resonant peak will flatten with increasing drive current.

A general rule of thumb is that a directly modulated laser can suppourt a bit rate of up to 1.2 times its relaxation oscillation frequency [2], however, the parasitics of device packaging and bonding can severely inhibit high frequency VCSEL performance [1]. VCSEL chip bonding introduces capacitance from the pads and resistance from the leads; it is typically modelled as a first order RC circuit [3]. The parasitics associated with packaged devices are more severe and tend to be represented by more complex circuit models [4], but they still act as low pass filters. Any attempt to measure the intrinsic response of a VCSEL will have to account for the parasitic effects of the packaging and bonding, and also the associated frequency response of measurement equipment and driving circuitry. This can be achieved through accurate circuit modelling of the parasitics, intelligent signal processing to remove the effects numerically, or the observation of phenomena related to the intrinsic device properties, which will be immune to the parasitic effects.

In the work that follows, the high speed characteristics of a VCSEL are examined and related rate equation parameters are extracted; special attention is paid to the design and effectiveness of each experiment performed.

II. Experimental Procedures

The high-speed characterisation of VCSELs requires great care in the experimental design stages, the precise implementation of, often complicated, procedures, and very accurate, well calibrated high speed instrumentation. As a result, frequency related measurements are very difficult to perform and often inconsistent [5]. A number of techniques exist to measure the intrinsic, high-frequency VCSEL characteristics, and extract the related parameters. Three different measurements are performed on a VCSEL with excellent single mode behaviour, to compare the consistency of results between techniques, immunity to parasitics, ease of measurement, and miscellaneous factors, such as the availability of equipment and speed of measurement.

A. Relative Intensity Noise

Even with a noise free current source, variations caused by spontaneous emission will be present in a VCSEL's steady-state output; these stochastic variations are referred to as relative intensity noise (RIN) [6]. The quantity of noise can be calculated by considering the relative amounts of DC (laser power) optical power to AC (noise power), Eq. (5) [7]:

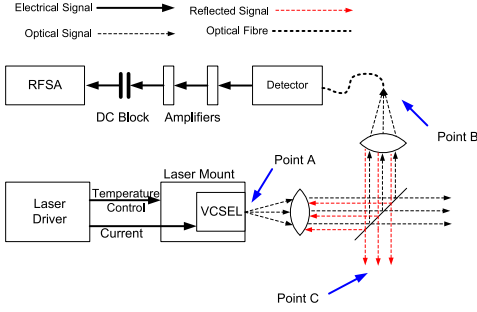$$RIN = \frac{\langle \delta P^2 \rangle}{\langle P \rangle^2} \qquad (5)$$

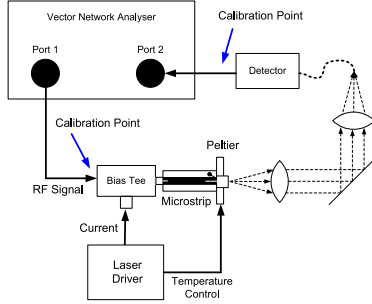Fig. 1: Setup used to measure the relative intensity noise.

Fig. 2: Setup used to measure VCSEL frequency response.

In addition to determining the noise performance of a laser, the RIN measurement can also be used to examine its high frequency properties - a peak in noise power is present at the resonant frequency [8]. This phenomena relates to the intrinsic VCSEL properties, and is unaffected by the packaging and bonding parasitics. Both the average noise power, and severity of the resonant noise peak decrease with increasing drive current. The RIN can be fitted to Eq. (6) to extract the resonant and damping frequencies.

$$RIN = \frac{A + B\omega^2}{\left(\omega^2 - \omega_r^2\right)^2 + \omega^2\Gamma_d^2} \quad (6)$$

Figure 1 shows the experimental setup employed to measure the relative intensity noise. The *Avalon 850SM LA* VCSEL is driven by a stable, constant current, and the light is coupled into a *Newport D-100-FC* high-speed photodetector. The average optical power can be measured directly, and the RF component is transmitted through a DC block and two low-noise amplifiers. The noise characteristic is recorded by a microwave spectrum analyser (*HP 8565E*); the spectral response of the detector, amplifiers, and the RFSA's noise floor can be numerically removed from these data to obtain the noise component of the VCSEL's output.

B. VNA Measurement

The small signal frequency response (S21) of the VCSEL (and associated circuitry) was measured with a vector network analyser (VNA). A constant drive current was supplied to the VCSEL and a low power modulating signal was generated by the VNA (*Rhode and Schwartz ZVCE*). The VCSEL's RF output was measured by a high speed photodetector and compared to the original modulating source. The relationship

between the two can be fitted to Eq. (1) to determine the resonant frequency and damping frequency of the VCSEL.

A bias tee is used to combine the RF and DC current sources; a $50\ \Omega$ microstrip provides matched, low loss signal transmission; temperature is controlled by a peltier, which is thermally isolated from all other components, Fig. 2.

While the values extracted from the RIN measurement and high resolution optical spectrum relate to the intrinsic VCSEL response, the S21 measurements implicitly contain package and bonding responses. These parasitics can be removed numerically, using the subtraction method suggested by [9]. The S21 of the VCSEL (and associated parasitics) at a reference drive current is subtracted from the response at other currents. It is assumed that the passive, parasitic elements are independent of current. The resultant magnitude response should be of the form:

$$\mathrm{Mag}(f) = \frac{f_{r_I}^4}{\left(f^2 - f_{r_I}^2\right) + \left(\Gamma_{d_I}/2\pi\right)^2 f^2} \times \\ \frac{\left(f^2 - f_{r_0}^2\right) + \left(\Gamma_{d_0}/2\pi\right)^2 f^2}{f_{r_0}^4} \quad (7)$$

where, f_{r_0} and Γ_{d_0} refer to the reference current and f_{r_I} and Γ_{d_I} refer to the response at current I.

C. High Resolution Optical Spectra

The phase noise of a laser is not spectrally flat, but instead has a resonance at the relaxation oscillation frequency [10] similar to the peak observed in the RIN spectrum. This resonance manifests itself as a pair of spectral side bands, adjacent to each lasing mode in the optical spectrum. Like the RIN measurement, the spacing of these sidebands is unaffected by package parasitics, and can be used to determine the intrinsic resonant frequency of a laser. However, the resonant frequency is so small in comparison to the optical lasing frequency that these side peaks are not resolvable by conventional optical spectrum analysers.

An extremely high finesse optical cavity (*Newport SR-240-CF Supercavity*) was employed to identify these side bands, Fig. 3. Light which passes through the resonator is measured by the photodetector, and amplified by a low noise voltage amplifier. The length of the cavity is varied by a periodic driving voltage applied to the actuators on the mirrors. The time dependent output of this optical bandpass filter can be measured on an oscilloscope, and from these data the spectral content of the beam can be determined.

III. RESULTS

A. Relative Intensity Noise

The RIN profile and fitted curve is shown for a drive currents of 3.1 mA, Fig. 4. The resonant peak can be observed , but an additional periodicity appears at higher drive currents, indicating the formation of an external cavity. The frequency separation of these peaks confirm the cavity exists between points *A* and *B* (as marked in Fig. 1). The cavity can be disrupted by inserting a tilted neutral density filter in the path
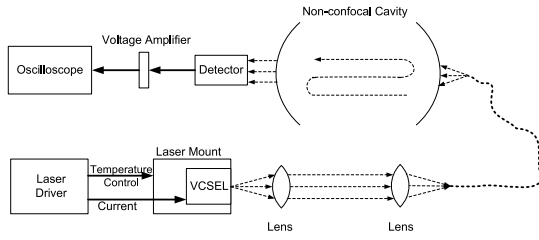
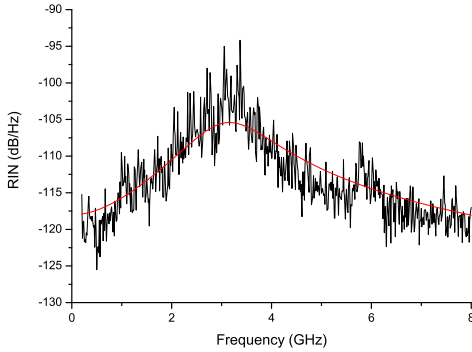Fig. 3: Setup used to obtain high-resolution, optical VCSEL spectra.

Fig. 4: Relative Intensity Noise at 3.1 mA drive current.

Fig. 5: Subtracted S21 response at 2.8 mA drive current.

Fig. 6: Output of the Supercavity for the VCSEL at 5 mA.

of the beam. Unfortunately, while a 10 dB optical attenuator removes the cavity effect, it also exacts a significant toll on the quality of the noise signal - the attenuated noise becomes almost unresolvable from the noise floor of the spectrum analyser. A reflected signal of approximately -15 dB relative to the emitted laser power was measured; Bae *et al.* report VCSELs can be exposed to feedback levels as high as -13 dB without experiencing significant changes in operation [11]. In this case, the external cavity obscures the features of the noise signal and complicates extraction procedures, but shouldn't affect the parameters being measured.

In accordance with the theory, the resonant peak is sharpest at currents close to threshold, and the RIN decreases as optical power increases. Both the resonant frequency and damping frequencies were extracted at each current. Figures 7 and 8 show the progression of the resonant frequency and damping frequency with current; the results very closely resemble the expected proportionality between f_r and $\sqrt{I - I_{th}}$. From the extracted parameters and Eq. (2), the carrier lifetime, τ_n, was found to be approximately 62.5 ps, and K was 0.3 ns.

B. VNA Measurement

The S21 response at 3.4 mA was chosen as the reference signal, and a multi-variable global parameter extraction was performed on the subtracted responses to obtain the resonant and damping frequencies of the VCSEL. A tilted optical attenuator can be used (in this case) to reduce reflections without sacrificing the sensitivity of the vector network analyser, however, additional resonances can still be observed in the subtracted S21 plots. As before, these reflections are of
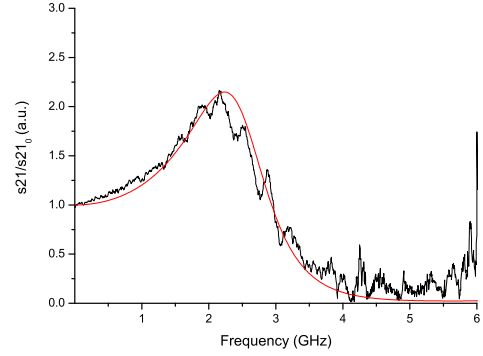
sufficient strength to complicate parameter extraction, but not strong enough to significantly alter VCSEL operation.

Figure 5 shows the resultant response of the VCSEL at 2.8 mA after the reference characteristic has been subtracted. The extracted resonant and damping frequencies are compared to the results from the other measurements in Fig. 7 and 8; τ_n was calculated as 68.1 ps and K = 0.34 ns.

C. High Resolution Optical Spectra

Figure 6 shows the recorded signal after the VCSEL beam has been passed through the supercavity. Resonant sidebands can be observed on either side of the main spectral peak (0 GHz relative frequency); the time original signal, measured in the time domain, can be converted to the frequency domain by calibrating with respect to the supercavity's known first transverse mode (28.66 GHz). The high resolution, optical spectra were recorded for a range of drive currents, and the extracted resonant frequencies are shown in Fig. 7. Over the current range shown, the side bands corresponding to the VCSEL's resonant frequency could be clearly identified. At lower drive currents, the emitted beam couldn't be coupled strongly enough into the cavity to resolve the bands; at higher currents, the side bands are too heavily damped to identify.
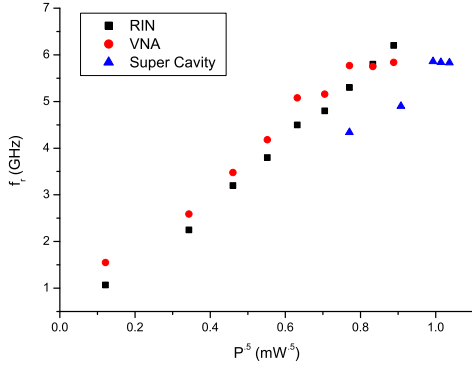
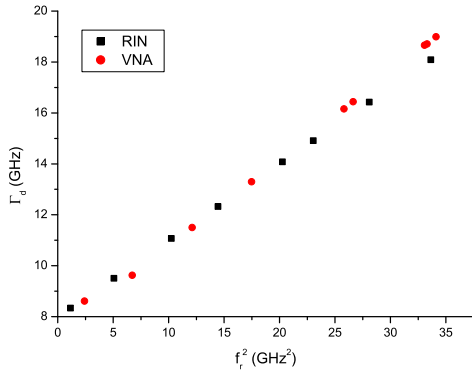Fig. 7: Measured resonant frequencies of the VCSEL.

Fig. 8: Measured damping frequencies of the VCSEL.

D. Comparison of Results

The resonant frequency is plotted against the square root of optical power of the fundamental mode, Fig. 7. The resonant frequency increases linearly with $\sqrt{P}$ in excellent agreement with the expected trend [12]:

$$f_r = D\sqrt{P} \qquad (8)$$

The parameter D was calculated as 6.93, 7.25, and 5.67 GHz/$\sqrt{\text{mW}}$ for the RIN, VNA, and super cavity measurements respectively. While the RIN and VNA measurements show outstanding correlation, the resonant frequencies measured by the supercavity are consistently slightly lower. The most likely explanation for this discrepancy is calibration - it is possible that the cavity transverse separation drifted from factory specification through time and use. A small variation between expected and actual separations would explain the uniform error seen in the results.

The damping frequencies, Γ_d, can also be extracted from the RIN and VNA measurements, Fig. 8, and they show the same excellent agreement.

IV. Discussion and Conclusions

Experiments have been performed to measure the resonant and damping frequencies using three different techniques: identification of the RIN peak, extraction from the S21 profile (as measured by the vector network analyser), and observation of the resonant side bands in the optical spectrum. Results for all three techniques were self consistent and in line with theory and previously noted experimental trends.

The S21 measurement is, in essence, *electrical*, and it inherits the familiar difficulties and requirements: well matched driving circuitry, low attenuation at all frequencies, and rigorous calibration conducted as close to the device as possible. By contrast, the super cavity provides an *optical* measurement; success relies heavily on alignment, mode matching, coupling power, and the quality of optical components. The RIN measurement falls somewhere in between - it measures a fundamental optical characteristic (spontaneous emission), but in the electrical domain. Through this fortunate combination, it is burdened little by either electrical or optical concerns.

In the final analysis, the super cavity measurement seems the most promising and underdeveloped; the VNA measurement, the most convenient and familiar; and the RIN measurement, the most robust.

References

[1] K. Petermann, *Laser Diode Modulation and Noise*. Kluwer Academic Publishers, 1991.

[2] J. E. Bowers, "High speed semiconductor laser design and performance," *Solid-St. Electron.*, vol. 30, no. 1, pp. 1–11, 1987.

[3] K. Czotscher, S. Weisser, A. Levin, and J. Rosenzweig, "Intensity modulation and chirp of 1.55-um multiple-quantum-well laser diodes: Modeling and experimental verification," *IEEE Select. Topics Quantum Electron.*, vol. 5, pp. 606–612, May/June 1999.

[4] M. Bruensteiner and G. C. Papen, "Extraction of VCSEL rate-equation parameters for low bias system simulation," *IEEE Select. Topics Quantum Electron.*, vol. 5, pp. 487–494, May/June 1999.

[5] G. Guekos, *Photonic Devices for Telecommunications: How to Model and Measure*. Berlin: Springer, 1999.

[6] K. Petermann, "External optical feedback phenomena in semiconductor lasers," *IEEE Select. Topics Quantum Electron.*, vol. 1, pp. 480–489, June 1995.

[7] G. E. Obarski and P. D. Hale, "How to measure relative intensity noise in lasers," *Laser Focus World*, pp. 273–277, 1999.

[8] D. M. Kuchta, J. Gamelin, J. D. Walker, J. Lin, K. Y. Lau, J. S. Smith, M. Hong, and J. P. Mannaerts, "Relative intensity noise of vertical cavity surface emitting lasers," *Appl. Phys. Lett.*, vol. 62, pp. 1194–1196, March 1993.

[9] P. A. Morton, T. Tanbun-Ek, R. A. Logan, A. M. Sergent, P. F. Sciortino, and D. L. Coblentz, "Frequency response subtraction for simple measurement of intrinsic laser dynamic properties," *IEEE Photon. Technol. Lett.*, vol. 4, pp. 133–136, 1992.

[10] S. Piazzolla, P. Spano, and M. Tamburrini, "Characterization of phase noise in semiconductor lasers," *Appl. Phys. Lett.*, vol. 41, pp. 696–696, 1982.

[11] J. W. Bae, H. Temkin, S. E. Swirhun, W. E. Quinn, P. Brusenbach, C. Parsons, M. Kim, and T. Uchida, "Reflection noise in vertical cavity surface emitting lasers," *Appl. Phys. Lett.*, vol. 63, pp. 1480–1482, 1993.

[12] M. C. Tatham, I. F. Lealman, C. P. Seltzer, L. D. Westbrook, and D. M. Cooper, "Resonance frequency, damping, and differential gain in $1.5\mu m$ multiple quantum-well lasers," *IEEE J. Quantum Electron.*, vol. 28, pp. 408–414, 1992.